Quantum trajectory Monte Carlo method describing the coherent dynamics of highly charged ions

Tatsuya Minami,[1] Carlos O. Reinhold,[2] and Joachim Burgdörfer[1,3]

[1]*Department of Physics and Astronomy,*
University of Tennessee, Knoxville, TN 37996-1200

[2]*Physics Division, Oak Ridge National Laboratory, Oak Ridge, TN 37831-6373*

[3]*Institute for Theoretical Physics, Vienna University of Technology, A-1040 Vienna, Austria*

(Dated: August 26, 2002)

Abstract

We present a theoretical framework for studying the dynamics of open quantum systems using a quantum Monte Carlo approach that can treat the build-up and time evolution of coherences. Our formalism provides a systematic path to derive the Monte Carlo algorithm starting from first principles. We employ a reduced density matrix approach in which the total system is divided into a system of interest and its environment. We derive a new Lindblad master equation for the time evolution of the reduced density matrix of the system that can be solved in terms of Monte Carlo sampling of quantum trajectories. We apply our method to study the coherence properties of the internal state of a Kr^{35+} ion subject to spontaneous radiative decay. Simulations exhibit clear signatures of coherent transitions.

PACS numbers: 34.50.Fa, 34.10.+x

I. INTRODUCTION

Investigations of "open quantum systems" are an attempt to apply quantum statistical mechanics to realistic complex problems. Even the most elementary system consisting of the internal electronic state of "free" one-electron ion/atom is an example of an open quantum system in contact with a "large reservoir". The reservoir refers here to the radiation field, which has an infinite number of degrees of freedom. The coupling between the system and the vacuum fluctuations of the radiation field triggers the spontaneous decay of the ion/atom and, in addition, it produces a shift of the electronic eigenstates, which is known as the Lamb shift. The internal electronic state of a fast ion traversing solids provides another example of an open quantum system in contact with a "large reservoir", which is given by the electronic and nuclear degrees of freedom of the solid. Moreover, for highly charged ions (HCIs) the coupling to the radiation field becomes comparable to the coupling to the particles in the solid [1, 2]. Therefore, any realistic description of the open quantum system should include both the radiation field and the degrees of freedom of the solid.

Theoretical analysis of open quantum systems is difficult not only because of the large number of degrees of freedom of the reservoir but also for the high-dimensional characteristics of the master equation of motion for the density matrix of the system [3–5]. If the density matrix is expanded in a set of N pure states of the system, the master equation is equivalent to a set of N^2 coupled equations involving N^4 couplings. Thus, computer storage for these couplings becomes a major bottleneck in the calculation of the dynamics of the system. In order to overcome this obstacle, quantum trajectory Monte Carlo (QTMC) techniques have been independently developed for fast ions traversing solids [2, 6, 7] and in quantum optics [8–10] for the description of few-state atomic systems interacting with the electromagnetic field. These developments were, however, incomplete to treat the time development of coherences between low-lying states of HCIs. In this work, we provide extension to QTMC methods used in quantum optics and ion-solid interactions. Our focus is on the transient build-up and destruction of coherences by stochastic processes. The main advancement compared to developments in quantum optics is that we go beyond the standard secular approximation [20, 21], which is incapable of describing the short time evolution of the coherences of the system. In turn, the main drawback of previous developments for ion-solid interactions is that they were strictly valid only for Rydberg states. Our extension

overcomes both limitations and provides a unified and general QTMC treatment describing the dynamics of open quantum systems. Due to space limitations, however, we provide here only examples for the coherent radiative decay of HCIs.

The basic idea involved in QTMC methods is that the reduced density matrix of the system can be constructed by Monte Carlo sampling of quantum trajectories, each of which is a solution of a non-linear stochastic Schrödinger equation (NLSSE). The QTMC solution for the reduced density matrix of the system follows a specific class of quantum master equations for the reduced density operator: the Lindblad equation [11, 12]. Therefore, an important prerequisite for the development of a QTMC method is the derivation of a realistic Lindblad master equation. Since the connection between the Lindblad equation and the original master equation it attempts to approximate is far from clear [13–18], our present derivation of a Lindblad equation is tested against a more reliable approximation. The starting point (or judge) of our derivation is the Redfield equation [19], which results from applying the Born-Markov approximation to the exact quantum master equation. We apply our QTMC method to study the time evolution of the internal state of Kr^{35+} subject to spontaneous radiative decay. We illustrate that the present Lindblad form allows the realistic description of coherences on a time scale corresponding to the inverse of the energy spacing between near-degenerate energy levels. Atomic units are used throughout.

II. THEORY

In this section we briefly review the basic properties of the Lindblad master equation and its solution by a quantum trajectory Monte Carlo method. A more comprehensive description can be found in Ref. [23]. We consider the interaction of a system (S) with a reservoir (R) which has a large number of degrees of freedom compared to those of the system. The total Hamiltonian is given by

$$H = H_S + H_R + V_{SR} \quad , \tag{2.1}$$

where V_{SR} describes the coupling between the system and the reservoir and H_S (H_R) is the internal Hamiltonian of the system (reservoir).

The time evolution of the density operator $\rho(t)$ of the system plus the reservoir is given by the Liouville-von Neumann equation,

$$i\rho(t) \;=\; [H,\, \rho(t)], \tag{2.2}$$

a solution of which is clearly out of reach for realistic systems. Instead, the focus is on the reduced density operator of the system, $\sigma(t)$, defined as

$$\sigma(t) \;=\; \mathrm{Tr_R}[\rho(t)] \tag{2.3}$$

where all degrees of freedom of the reservoir is traced out. Formulating a master equation of motion for σ is a difficult task. The approach proposed by Lindblad starts by postulating an equation based on the principle that the time evolution of σ should be a unitary mapping of the system Hilbert space onto itself preserving complete positive definiteness. The reduced dynamics in the system is therefore described by

$$\begin{aligned} \frac{d}{dt}\sigma(t) \;&=\; -i[H_S, \sigma(t)] - \frac{1}{2}\sum_k \Big[S^\dagger(k)S(k)\sigma(t) \\ &+\; \sigma(t)\, S^\dagger(k)S(k) \,-\, 2\, S(k)\, \sigma(t)\, S^\dagger(k)\Big] \end{aligned} \tag{2.4}$$

In (2.4) we have labeled the Lindblad jump operators $S(k)$ by the index k, which represents the degrees of freedom associated with the reservoir. In our application below this will express the direction of polarization of the photons.

The physical significance of (2.4) has been extensively debated in the literature (see e.g. [13, 15, 18]. We take (2.4) as a useful approximation for the dynamics of the open quantum systems on time scales that are large compared to the relaxation time of the reservoir but are comparable to the time scale for the evolution of the system degrees of freedom where expectation values of observables can meaningfully be extracted. The importance of the Lindblad equation in the present context is the mapping onto a non-linear stochastic Schrödinger equation (for details see [11]), which can be solved by a quantum trajectory Monte Carlo (QTMC) technique. Accordingly, the density operator of the system can be constructed from the evolution of an ensemble of N_{traj} pure states

$$\sigma(t) \;=\; \frac{1}{N_{traj}} \sum_{\eta=1}^{N_{traj}} |\Psi^\eta(t)\rangle\langle\Psi^\eta(t)| \tag{2.5}$$

where η labels the different stochastic realizations of quantum trajectories $|\Psi^\eta(t)\rangle$. Such an expression for $\sigma(t)$ tacitly assumes that an initial ensemble can be uniquely defined

irrespective of its coupling to the reservoir. Obviously, preservation of positive definiteness is a condition for the existence of the mapping onto an incoherent superposition of state probabilities (2.5). The time evolution of $|\Psi^\eta(t)\rangle$ is given by a NLSSE. Alternatively, it can be calculated by constructing the corresponding time evolution operator $U^\eta(t,0)$ (defined by $|\Psi^\eta(t)\rangle = U^\eta(t,0)|\Psi^\eta(0)\rangle$), which can be decomposed into a sequence of products of two types of evolution operators

$$U^\eta(t,0) = U^\eta_{cont}(t,t_n)\prod_{j=1}^{n} U^\eta_{jump}(k_j,t_j)U^\mu_{cont}(t_j,t_{j-1}) \quad ,(t_0=0). \tag{2.6}$$

One factor, $U^\eta_{jump}(k_j,t_j)$, represents a discontinuous change of the wavefunction, a stochastic jump, at randomly chosen times $t = t_j$ and indexes k_j. The other factor, $U^\eta_{cont}(t_{j+1},t_j)$, stands for a continuous change of the wavefunction during the time period $[t_{j+1},t_j]$ between stochastic "jumps". The obvious technical advantage of the mapping of the Lindblad master equation onto (2.6) is that memory storage with the dimension of the state space of the system as N^2 rather than with N^4 for the direct solution of the Lindblad equation. Clearly, the price to pay is the additional scaling with N_{traj}, i.e. the number of trajectories required to control the statistical error of the ensemble solution.

The basic ingredients of the Monte Carlo algorithm are therefore random jump times t_j and indexes k_j, the continuous evolution operators U^η_{cont}, and the jump operators U^η_{jump}. The continuous time evolution of the wavefunction during a time interval between two jumps is given by

$$|\Psi^\eta(t_j)\rangle = U^\eta_{cont}(t_j,t_{j-1})\,|\Psi^\eta(t_{j-1})\rangle = \frac{\exp\left[-iH_{eff}(t_j-t_{j-1})\right]|\Psi^\eta(t_{j-1})\rangle}{||\exp\left[-iH_{eff}(t_j-t_{j-1})\right]|\Psi^\eta(t_{j-1})\rangle||}\,, \tag{2.7}$$

with

$$H_{eff} = H_S - \frac{i}{2}\sum_k S^\dagger(k)\,S(k) \tag{2.8}$$

being an effective, non-hermitian Hamiltonian that includes the effect of decay due to the coupling to the reservoir[11]. The continuous evolution operator accounts for the first two terms of the Lindblad equation.

Quantum jumps at times t_j for a given value of k_j are described by the operators

$$|\Psi^\eta(t_j+\delta t)\rangle \;=\; U^\eta_{jump}(k_j,t_j)\,|\Psi^\eta(t_j)\rangle \;=\; \frac{S(k_j)\,|\Psi^\eta(t_j)\rangle}{||S(k_j)\,|\Psi^\eta(t_j)\rangle||} \tag{2.9}$$

where $\delta t \to 0$ is an infinitesimal time step. The jump operator simulates the effect of the last term of the Lindblad equation. The jump times t_j and indexes k_j are sampled at random from a probability density such that when the quantum trajectory is in a state $|\Psi^\eta(t)\rangle$ the average number of jumps per infinitesimal time step dt is $\overline{dN_k(t)} = dt\langle\Psi^\eta(t)|S^\dagger(k)S(k)|\Psi^\eta(t)\rangle$

Up to this stage, the Lindblad jump operator $S(k)$ is unknown. In order to determine this operator, one needs to analyze the approximate reduction of the quantum master for the density matrix of the system to a Lindblad form. We emphasize that such a reduction is not unique. The starting point of our analysis is the Redfield equation [19], which is obtained from the exact master equation after using the Born-Markov approximation. The figure of merit for our Lindblad approximation is the degree to which the resulting density matrix is capable of reproducing the time evolution of atomic coherences on time scales long compared to the reservoir correlation time, τ_c, but short compared to the time scale of the secular motion of the atomic population. Such an analysis appears to be missing for true multi-state problems.

The Redfield equation for the reduced density matrix of the system can be written as

$$\begin{aligned}\frac{\partial}{\partial t}\sigma_{\alpha\beta}(t) &= -i\omega_{\alpha\beta}\,\sigma_{\alpha\beta}(t) - \frac{1}{2}\sum_k\sum_{\nu,\mu=1}^{N}\Big[X^\dagger_{\alpha\nu}(k)Y_{\nu\mu}(k)\sigma_{\mu\beta}(t)\\ &+ \sigma_{\alpha\nu}(t)\,Y^\dagger_{\nu\mu}(k)X_{\mu\beta}(k) - Y_{\alpha\nu}(k)\,\sigma_{\nu\mu}(t)X^\dagger_{\mu\beta}(k) - X_{\alpha\nu}(k)\,\sigma_{\nu\mu}(t)Y^\dagger_{\mu\beta}(k)\Big] \quad (2.10)\end{aligned}$$

where the indexes $\alpha, \beta, ...$ denote the eigenstates of H_S (i.e. $H_S|\alpha\rangle = |\alpha\rangle\epsilon_\alpha$) and $\omega_{\alpha\beta} = \epsilon_\alpha - \epsilon_\beta$. The reason why the Redfield equation is not the same as the Lindblad equation (2.4) is that the X and Y operators are not the same. In fact,

$$Y_{\nu\mu}(k) = X_{\nu\mu}(k)\;\chi(k,\omega_{\mu\nu}) \quad (2.11)$$

where $\chi(k,\omega)$ is directly related to the imaginary part of the susceptibility of the reservoir.

The crucial point is now that the Redfield equation does not possess the same structure as the Lindblad equation (2.4). Mapping Eq.(2.10) onto a Lindblad form requires additional approximations which have profound consequences as to the regime within which the Lindblad equations can be applied. The standard approximation involved is the so-called "secular approximation" [20, 21] (also referred to as the rotating wave approximation). If we transform Eq. (2.10) to the interaction picture, all terms on the right hand side carry

oscillatory phase factors of the form $exp(i\omega_{\alpha\beta}t)$. The secular approximation assumes that all terms average out unless the phase is identically zero (i.e. $exp(i\omega_{\alpha\beta}t)$ is replaced by $\delta_{0,\omega_{\alpha\beta}}$). If the energy spectrum of the system is non-degenerate, the secular approximation yields a Lindblad form (2.4) with a jump operator

$$S^{sec}_{\alpha\beta}(k) = \delta_{\alpha\beta}(k)\ X_{\alpha\beta}(k)\ \sqrt{\chi(k,\omega_{\beta\alpha})} \tag{2.12}$$

The secular approximation does not allow for the production of coherences between different energy eigenstates due to the interaction with the environment but allows only for its decay. This result is, however, only valid for the long time scale $t \gg T_I = 2\pi/|\omega_{\alpha\beta}|$. On an intermediate time scale $\tau_c \ll t \leq T_I$, the build-up of transient coherences can occur but has been mostly ignored in the context of Lindblad equations. In order to develop a Lindblad form that can be applied in this intermediate time regime, we define the jump operator $S_{\alpha\beta}(k)$ as the geometric mean of $X_{\alpha\beta}(k)$ and $Y_{\alpha\beta}(k)$, i.e.,

$$S_{\alpha\beta}(k) = \sqrt{X_{\alpha\beta}(k)Y_{\alpha\beta}(k)} = X_{\alpha\beta}(k)\ \sqrt{\chi(k,\omega_{\beta\alpha})} \tag{2.13}$$

This result represents a simple but useful generalization of the secular approximation. In the next section we apply this generalization to the radiative decay of a HCI and show that it provides an accurate algorithm to calculate the build-up of coherences in the time regime $t \lesssim T_I$

III. APPLICATION AND CONCLUSIONS

In the case of a one-electron ion interacting with the vacuum fluctuations of the electromagnetic field, the system is the internal electronic state of the ion and the total Hamiltonian (2.1) is

$$H_S \equiv -\frac{\nabla^2_{\vec{r}}}{2} - \frac{Z_p}{r} + \Delta H_{rel} \tag{3.1}$$

where $\vec{r} = (r_1, r_2, r_3)$ is the position coordinate of the electron, Z_p is charge of the ion, and ΔH_{rel} represents relativistic and Lamb-shift corrections. The eigenstates of H_S can be expressed as $|\alpha\rangle = |n\,l\,j\,m_j\rangle$ where n is the principal quantum number, l is the orbital angular momentum, and j and m_j are the total angular momentum and its projection onto

the z-axis. The interaction between the system and the reservoir V_{SR} can be wrriten as the product

$$V_{SR}(\vec{r}) = \frac{i}{c}\vec{A} \cdot \nabla_{\vec{r}}, \tag{3.2}$$

where $\vec{A}$ is the vector potential. In the dipole approximation $\vec{A}$ does not act on the electron and one obtains $X_{\alpha\beta}(k) = \langle\alpha|r_k|\beta\rangle$ and $\chi(k, \omega_{\beta\alpha}) = \omega^3_{\beta\alpha}$.

The physics of the radiative decay process for a Kr^{35+} ion is illustrated in Figs 1-4. In Figs. 1 and 2 the ion is initially prepared at $t = 0$ in the $|4p_{3/2,1/2}\rangle$ state. The first figure displays contour plots of the relative coherences

$$Q_{\alpha\beta} = \frac{|\sigma_{\alpha\beta}|}{\sqrt{\sigma_{\alpha\alpha}\sigma_{\beta\beta}}} \tag{3.3}$$

on the α-β plane (for $\sigma_{\alpha\alpha} < 10^{-10}$ or $\sigma_{\beta\beta} < 10^{-10}$ we set $Q_{\alpha\beta} = 0$). Note that all diagonal elements $Q_{\alpha\alpha}$ are equal to unity (unless $\sigma_{\alpha\alpha} < 10^{-10}$), and, therefore, the figure does not provide a quantitative measure of the time evolution of the populations. Since density matrices have the property $|\sigma_{\alpha\beta}| \leq \sqrt{\sigma_{\alpha\alpha}\sigma_{\beta\beta}}$, the relative coherence takes values in the interval $0 < Q_{\alpha\beta} < 1$. If the system is in a pure state, all off-diagonal relative coherences of populated states are equal to unity. Finite relative coherences smaller than unity imply that the system is in a partially coherent state.

Direct decay channels for the electron initially in the $|4p_{3/2,1/2}\rangle$ state are the $1s$, $2s$, $3s$ and $3d$ states. $2p$ levels are populated slowly and indirectly via the decay of the $3s$ or $3d$ states. A remarkable aspect of the direct radiative decay from a single initial state is that unless a measurement is taken to determine the state of the emitted photon, the system decays into a partially coherent superposition of states. Inter-shell coherences (different n quantum numbers) are rapidly washed out as a consequence of their large level splitting $\omega_{\alpha\beta}$ (i.e. the natural decoherence time $T_I = 2\pi/\omega_{\alpha\beta}$ is very small). Therefore, in the following we focus on the $3s$-$3d$ and $3d$-$3d$ coherences. The most striking feature in figure 1 is the transient build-up of off-diagonal elements ($3s$-$3d$ and $3d$-$3d$ coherences) at short times $t < T_I$ and their successive decay at much longer times $t \gg T_I$. Such features are absent in the standard secular approximation.

In order to verify the accuracy of the proposed jump operator ((2.13)) entering the Lindblad form, we compare in Fig. 2 the time evolution of selected density matrix elements with

the result obtained solving the full Redfield equation (2.10) as well as that of the Lindblad equations using the standard secular approximation ((2.12)). For the diagonal elements describing the population of the $3s_{1/2,-1/2}$ and $3d_{3/2,-1/2}$ states all three approximations agree well with each other. However, only our Lindblad form can reproduce the transient build-up of coherence due to the spontaneous decay as predicted by the Redfield equation. The secular approximation, by construction, fails. Coherences begin to be damped out for times $t > t_I = 2\pi/|\omega_{3s,3d}| = 7.6$a.u. Nevertheless, smaller non-varnishing coherences can be observed even beyond t_I, the reason being that the lifetime of the "feeder" state is even longer and continuously replenishes the coherence. The point to be noted is that the standard secular approximation fails even for times longer than t_I and up to the lifetime of the feeder state. It is therefore completely inadequate for the entire transient regime.

In Figs. 3 and 4 we provide another example of coherent radiative decay for which the system is initially prepared in a coherent superposition of the $3s_{1/2,-1/2}$ and $3p_{1/2,-1/2}$ states: $|\Psi(0)\rangle = (|3s_{1/2,-1/2}\rangle + |3p_{1/2,-1/2}\rangle)/\sqrt{2}$. The contour plots in Fig. 3 illustrate the different time scales involved in the time evolution of this problem within the $n = 2$ shell. At $t = 0.2a.u.$ the ion has decays into a partially coherent superposition of most states in this shell. At $t = 2$ coherences between the $2p_{3/2}$ and $2p_{1/2}$ vanish since this time is close to the decoherence time given by the fine structure splitting. Finally, at $t = 210a.u.$, even the coherence between $2p_{1/2}$ and $2s_{1/2}$ states vanishes because the propagation time is longer than the decoherence time given by the Lamb shift ($\sim 99a.u.$). Figure 4 shows (much like Fig. 2) that the proposed generalization of the jump operator (2.13) provides an excellent approximation for the description of the production and destruction of coherences due to radiative decay.

In summary, we have derived from first principles a general formalism based on the Lindblad equation and its quantum trajectory Monte Carlo implementation to describe the dynamics of open quantum systems. Compared to other work in this field, the main development introduced in this article is that we go beyond the secular approximation and we provide a method that gives good account for the short time evolution of the coherences of the system.

Acknowledgments

This work was supported by the NSF and FWF (Austria). COR acknowledges support by the DCS, OBES, USDOE, managed by UT-Battelle, LLC, under contract DE-AC05-00OR22725.

---

[1] D. Vernhet, J.P. Rozet, E. Lamour, B. Gervais, C. Fourment, and L.J. Dubé, Phys. Script. **T80A**, 83 (1999).

[2] T. Minami, C.O. Reinhold, M. Seliger, J. Burgdörfer, C. Fourment, B. Gervais, E. Lamour, J-P. Rozet, and D. Vernhet, Phys. Rev. A., **65** 032905 (2002)

[3] R. Zwanzig, J. Chem. **33**, 1338 (1960).

[4] J. Prigogine and P. Resibois, Physica **27**, 629 (1961).

[5] H. Gabriel, Phys. Rev. **181**, 506 (1969).

[6] J. Burgdörfer and J. Gibbons, Phys. Rev. A, **42**, 1206 (1990).

[7] D. G. Arbó, C. O. Reinhold, S. Yoshida, and J. Burgdörfer, Nucl. Inst. & Methods Phys. Res. B, **164-165** 495 (2000).

[8] J. Dalibard, Y Castin, and K. Mølmer, Phys. Rev. Lett., **68**, 580(1992); K. Mølmer, Y Castin, and J. Dalibard, J. Opt. Soc. Am. B, **10**, 524 (1993)

[9] R. Dum, P. Zoller and H. Ritsch, Phys. Rev. A, **45**, 4879 (1992).

[10] J. Carmichael, Phys. Rev. Lett., **70** 2273 (1993).

[11] C. W. Gardiner and P. Zoller, *Quantum Noise* (Springer, 1999).

[12] G. Lindblad, Commun. Math. Phys. **48** 119 (1976); G. Lindblad, Rep. Math. Phys., **10** 393 (1976).

[13] U. Weiss, Quantum Dissipative Systems, World Scientific (Singapore, 1999).

[14] L. Diosi, Europhys. Lett. **22**, 1 (1993).

[15] A. Suarez, R. Silbey, and I. Oppenheim, J. Chem. Phys. **97**, 5101 (1992).

[16] W. Pollard and R. Friesner, J. Chem. Phys. **100**, 5054 (1994).

[17] P. Pechukas, Phys. Rev. Lett. **73**, 1060 (1994).

[18] D. Kohen, C. Marston, and D. Tannor, J. Chem. Phys. **107**, 5236 (1997).

[19] A.G. Redfield, IBM J. Res. Dev. **1**, 19 (1957); Adv. Magn. Reson. **1**, 1 (1965).

[20] C. Cohen-Tannoudji, J. Dupont-Roc, and G. Grynberg, 'Atom-Photon Interactions', Wiley Interscience (1992)

[21] K. Blum, *Density Matrix Theory and Applications*, Plenum, NY, 1981).

[22] R. Blümel, A. Buchleitner, R. Graham, L. Sirko, U. Smilansky, H. Walther, *Phys. Rev. A* **44**, 4521 (1991).

[23] T. Minami, C.O. Reinhold, and J. Burgdörfer, submitted to Phys. Rev. A.

FIG. 1: Contour plots of relative coherences of the reduced density matrix of a free standing Kr^{35+} ion that radiatively decays for various propagation times as a function of the state index. The system is initially prepared in the pure state $|\psi(0)\rangle = |4p_{3/2,1/2}\rangle$. For visual clarity, we only plot the matrix elements involving $m_j > 0$ states.

FIG. 2: Comparison of selected elements of the reduced density matrix of a free standing Kr^{35+} ion that radiatively decays calculated using three different methods. The system is initially prepared in the pure state $|\psi(0)\rangle = |4p_{3/2,1/2}\rangle$. The figure displays (a) the populations of the $3s_{1/2,-1/2}$ and $3d_{3/2,-1/2}$ states, and (b) their relative coherence.

FIG. 3: Contour plots of relative coherences of the reduced density matrix of a free standing Kr^{35+} ion that radiatively decays for various propagation times as a function of the state index. The system is initially prepared in the pure $|\psi(0)\rangle = (|3s_{1/2,-1/2}\rangle + |3p_{1/2,-1/2}\rangle)/\sqrt{2}$

FIG. 4: Comparison of selected elements of the reduced density matrix of a free standing Kr^{35+} ion that radiatively decays calculated using three different methods. The system is initially prepared in the pure state $|\psi(0)\rangle = (|3s_{1/2,-1/2}\rangle + |3p_{1/2,-1/2}\rangle)/\sqrt{2}$. The figure displays (a) the populations of the $2s_{1/2,-1/2}$ and $2p_{1/2,-1/2}$ states, and (b) their relative coherence.

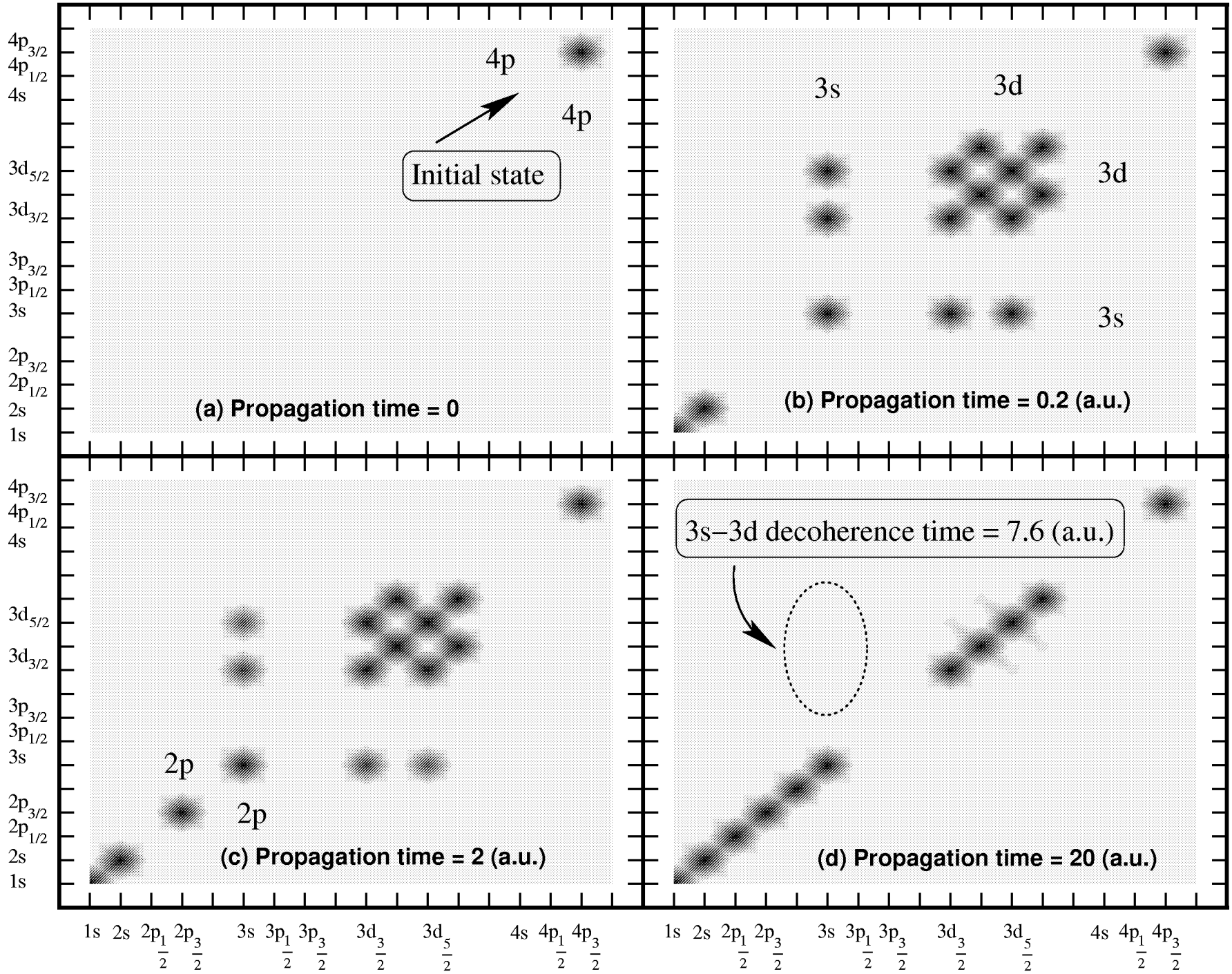
4p
4p
Initial state
(a) Propagation time = 0
3s
3d
3d
3s
(b) Propagation time = 0.2 (a.u.)
2p
2p
(c) Propagation time = 2 (a.u.)
3s–3d decoherence time = 7.6 (a.u.)
(d) Propagation time = 20 (a.u.)
4p3/2 4p1/2 4s 3d5/2 3d3/2 3p3/2 3p1/2 3s 2p3/2 2p1/2 2s 1s
1s 2s 2p1/2 2p3/2 3s 3p1/2 3p3/2 3d3/2 3d5/2 4s 4p1/2 4p3/2

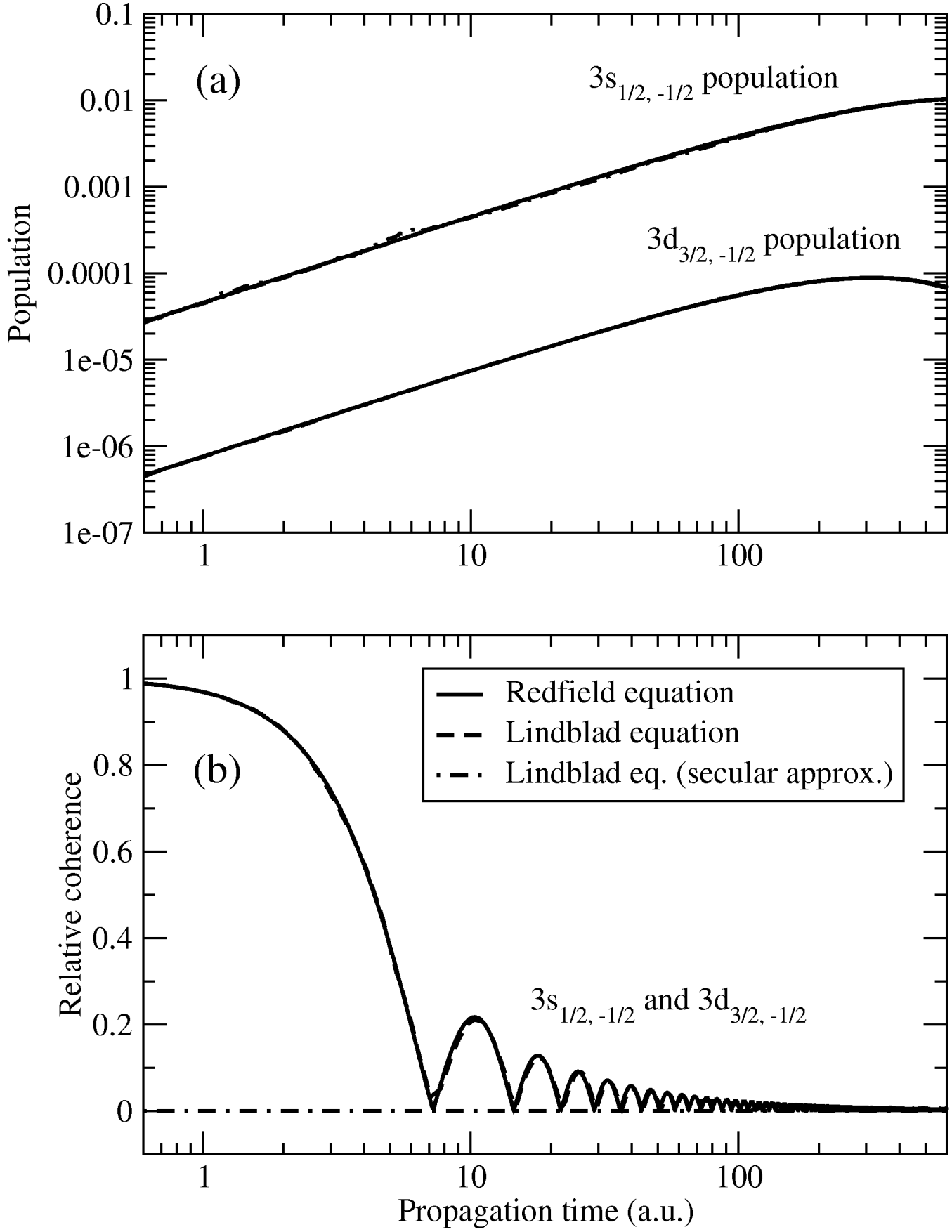
(a)
3s1/2, -1/2 population
3d3/2, -1/2 population
Population
0.1
0.01
0.001
0.0001
1e-05
1e-06
1e-07
1
10
100
(b)
Redfield equation
Lindblad equation
Lindblad eq. (secular approx.)
3s1/2, -1/2 and 3d3/2, -1/2
Relative coherence
1
0.8
0.6
0.4
0.2
0
1
10
100
Propagation time (a.u.)

Fig. 2

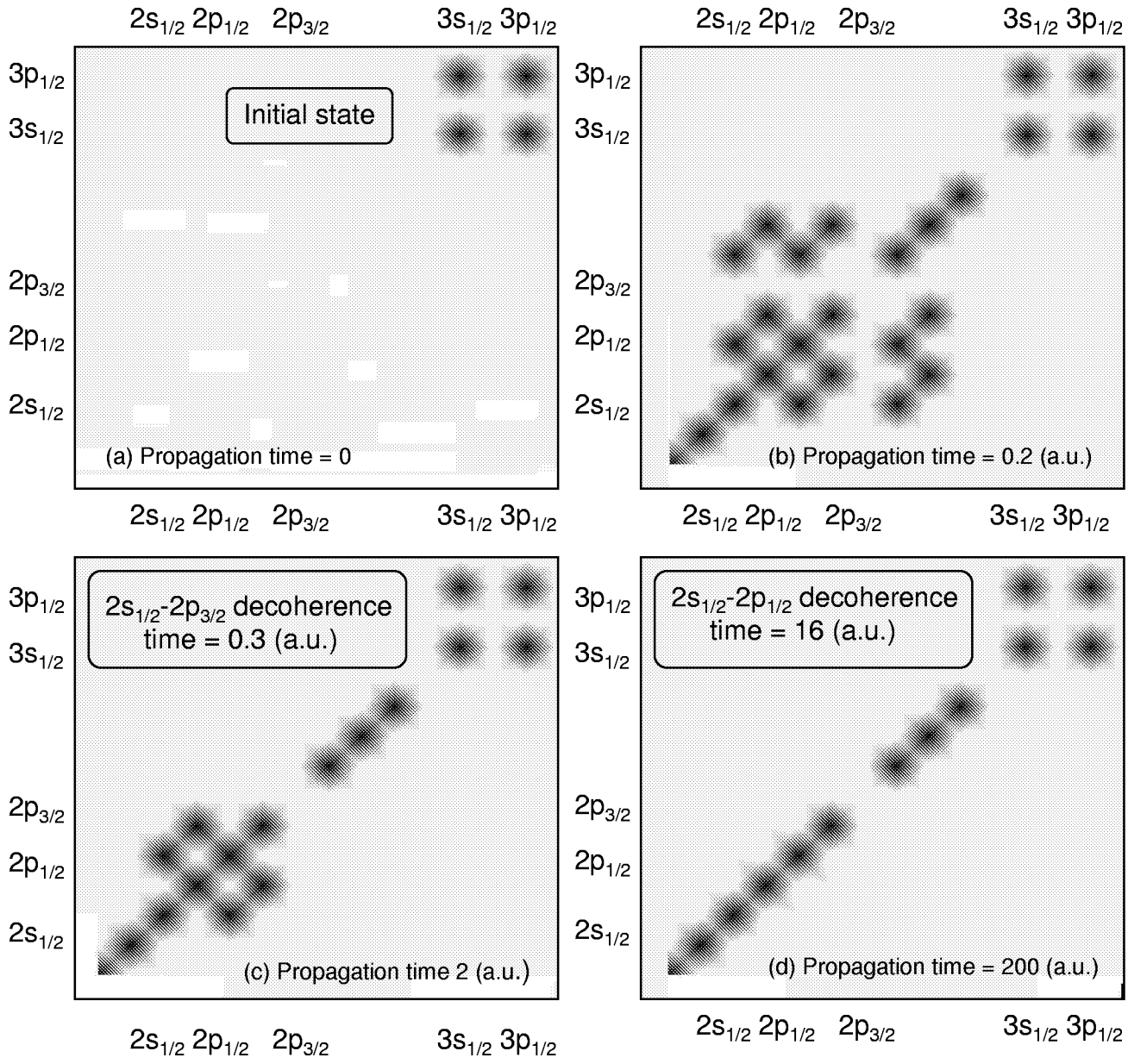
2s1/2 2p1/2 2p3/2 3s1/2 3p1/2
3p1/2
3s1/2
2p3/2
2p1/2
2s1/2
Initial state
(a) Propagation time = 0
(b) Propagation time = 0.2 (a.u.)
2s1/2-2p3/2 decoherence time = 0.3 (a.u.)
(c) Propagation time 2 (a.u.)
2s1/2-2p1/2 decoherence time = 16 (a.u.)
(d) Propagation time = 200 (a.u.)

Figure 3

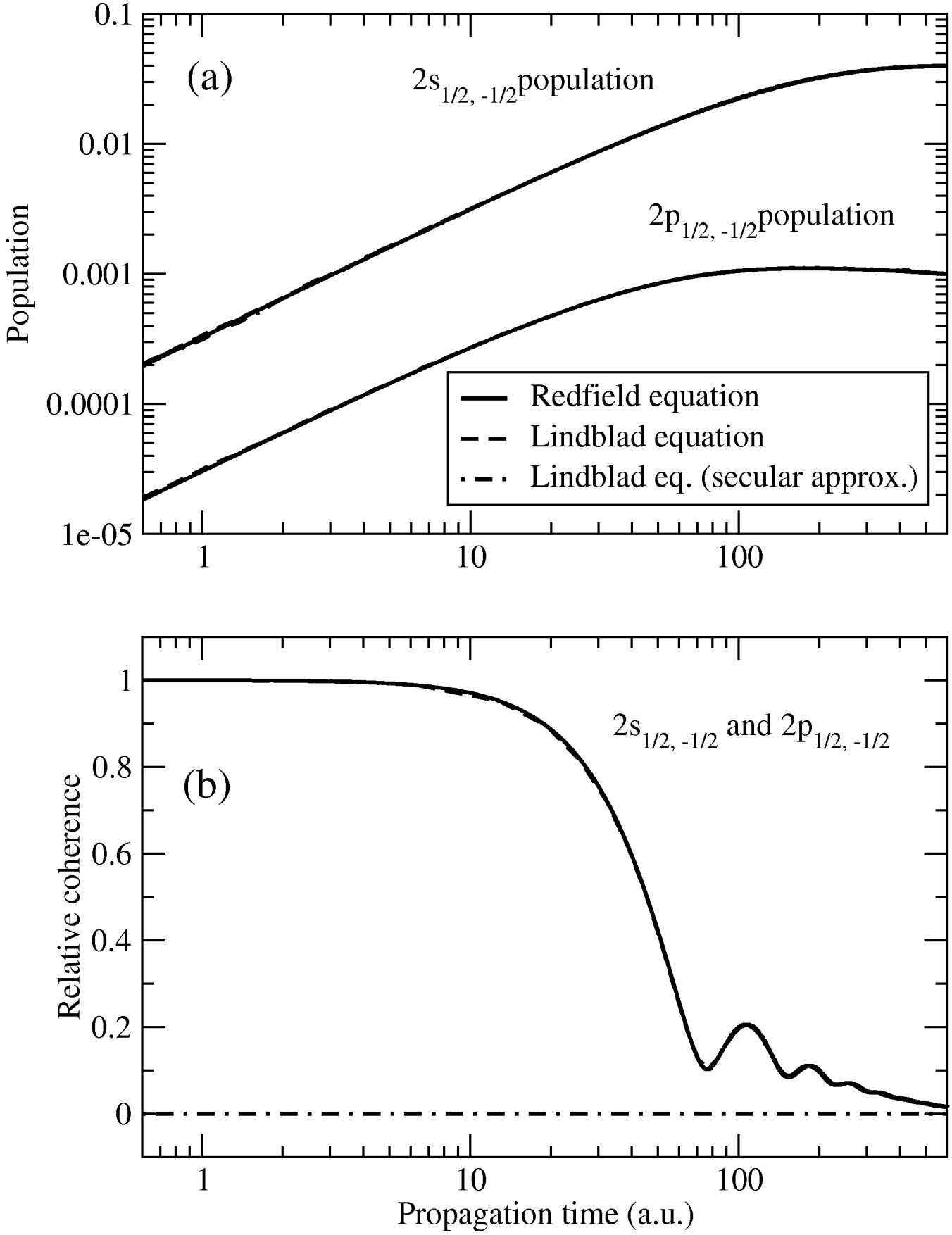
(a)
$2s_{1/2,\,-1/2}$population
$2p_{1/2,\,-1/2}$population
Population
0.1
0.01
0.001
0.0001
1e-05
1
10
100
Redfield equation
Lindblad equation
Lindblad eq. (secular approx.)
(b)
$2s_{1/2,\,-1/2}$ and $2p_{1/2,\,-1/2}$
Relative coherence
1
0.8
0.6
0.4
0.2
0
1
10
100
Propagation time (a.u.)

Fig. 4